



Microscopic description of heavy ion collisions around the barrier

Cédric Simenel, Benoît Avez, Cédric Golabek

► To cite this version:

Cédric Simenel, Benoît Avez, Cédric Golabek. Microscopic description of heavy ion collisions around the barrier. KERNZ08, Dec 2008, Queenstown, New Zealand. pp.0. hal-00376251

HAL Id: hal-00376251

<https://hal.science/hal-00376251>

Submitted on 17 Apr 2009

HAL is a multi-disciplinary open access archive for the deposit and dissemination of scientific research documents, whether they are published or not. The documents may come from teaching and research institutions in France or abroad, or from public or private research centers.

L'archive ouverte pluridisciplinaire **HAL**, est destinée au dépôt et à la diffusion de documents scientifiques de niveau recherche, publiés ou non, émanant des établissements d'enseignement et de recherche français ou étrangers, des laboratoires publics ou privés.

Microscopic description of heavy ion collisions around the barrier

Cédric Simenel and Benoît Avez

CEA, Centre de Saclay, IRFU/Service de Physique Nucléaire, F-91191 Gif-sur-Yvette, France.

Cédric Golabek

GANIL (IN2P3/CNRS - DSM/CEA), BP 55027, F-14076 Caen Cedex 5, France.

(Dated: April 17, 2009)

A microscopic mean-field description of heavy ion collisions is performed in the framework of the time dependent Hartree-Fock theory using a Skyrme energy density functional. A good agreement with experiments is obtained on the position of the fusion barriers for various total masses and mass asymmetries. The excitation function of the $^{16}\text{O}+^{208}\text{Pb}$ is overestimated by about 16% above the barrier. Transfer below the barrier is studied in $^{16}\text{O}+^{208}\text{Pb}$ central collisions. Heavier systems are considered to study their fusion hindrance. We also compute collision times of the $^{238}\text{U}+^{238}\text{U}$ system. The latter has been used to produce super-strong electric fields and to test non perturbative quantum electrodynamics theory. Indeed, if the life time of such giant system is of the order of few 10^{-21} s, its electric field should induce spontaneous electron-positron pair emissions from vacuum. In our calculations, highest collision times are reached in the $^{238}\text{U}+^{238}\text{U}$ reaction for center of mass energies between 1000 and 1300 MeV.

I. INTRODUCTION

Description of nuclear reactions is very challenging, especially at energies around the fusion barrier generated by the competition between Coulomb and nuclear interactions. It has been established that the structure of the collision partners may affect strongly the reaction mechanisms in this energy domain, as, for instance, the fusion cross-sections (for a review, see, e.g., Ref. [1]). In fact, a good understanding of these effects is crucial for the quest of superheavy elements (SHE) [2]. Indeed, different structures of the collision partners may change SHE production cross sections by several orders of magnitudes [3]. For instance, fusion hindrance has been observed for collisions of quasisymmetric heavy systems with typical charge products $Z_1 \times Z_2 \geq 1600$ [4]. Here, dynamical shape evolution of the dinuclear system and transfer between fragments are expected to play a significant role on this fusion hindrance. Investigations on collision dynamics between actinides are also of interest, in particular to study the physics of superstrong electric fields [5, 6, 7].

It is therefore recommended to treat both structure of nuclei and their collision dynamics within the same formalism. This is the case of fully microscopic approaches such as the time dependent Hartree-Fock (TDHF) theory proposed by Dirac in 1930 [8]. This time dependent version of the well known Hartree-Fock (HF) theory [9, 10] gives a self-consistent mean-field description of nuclear dynamics. The success of the first HF calculations based on Skyrme interactions [11, 12] led to tremendous activities to describe nuclear structure within mean-field based approaches (see, e.g., Ref. [13] for a review). Early TDHF calculations in nuclear physics [14, 15] have been done with the seek for a description of the dynamics of nuclei as good as their static properties [16]. At that time, theoreticians had to use various symmetries and simplified Skyrme interactions to reduce computational

times. Now, recent increase of computational power allowed realistic TDHF calculations of nuclear collisions in 3 dimensions with full Skyrme energy density functional (EDF) [17, 18].

In this proceeding, we present a review of various TDHF studies of heavy ion collisions. In Section II, we recall the formalism and detail the calculation. In Section III, we study fusion and transfer in light and medium heavy systems. In particular, a detailed study of the $^{16}\text{O}+^{208}\text{Pb}$ reaction is presented. In Section IV, we investigate the problem of fusion hindrance of heavy quasisymmetric systems. Then, we study the collision time of two ^{238}U nuclei in Section V before to conclude.

II. THE TIME-DEPENDENT HARTREE-FOCK APPROACH

In nuclear physics, the TDHF theory is applied with a Skyrme EDF modeling nuclear interactions between nucleons [11]. The EDF is the only phenomenological ingredient of the model, as it has been adjusted on nuclear structure properties like infinite nuclear matter and radii and masses of few doubly magic nuclei [19]. The main approximation of the theory is to constrain the many-body wave function to be an antisymmetrized independent particles state at any time. The latter ensures an exact treatment of the Pauli principle during time evolution. Though TDHF does not include two-body collision term, it is expected to treat correctly one-body dissipation which is known to drive low energy reaction mechanisms as Pauli blocking prevents nucleon-nucleon collisions.

The main advantage of TDHF is that it treats static properties *and* dynamics of nuclei within the same formalism and the same EDF. The initial state is obtained through static HF calculations which give a good approximation of nuclear binding energies and deformations.

Another important advantage of TDHF for near-barrier reaction studies is that it contains all types of couplings between the relative motion and internal degrees of freedom whereas in coupled channels calculations one has to include them explicitly according to physical intuition. However, TDHF gives only classical trajectories for the time-evolution and expectation values of one-body observables. In particular, it does not include tunneling of the many-body wave function.

Inclusion of pairing correlations responsible for superfluidity in nuclei have been done recently within the time dependent Hartree-Fock-Bogolyubov theory to study pairing vibrations in nuclei [20]. However, realistic applications to heavy ion collisions are not yet achieved and are beyond the scope of this work.

A. Formalism

The TDHF equation can be written as a Liouville-Von Neumann equation

$$i\hbar \frac{\partial}{\partial t} \rho = [h[\rho], \rho] \quad (1)$$

where ρ is the one body density matrix associated to the total independent particles state with elements

$$\rho(\mathbf{r}s q, \mathbf{r}'s' q') = \sum_{i=1}^{A_1+A_2} \varphi_i(\mathbf{r}s q) \varphi_i^*(\mathbf{r}'s' q'). \quad (2)$$

The sum runs over all occupied single particle wave functions φ_i and \mathbf{r} , s and q denote the position, spin and isospin of the nucleon respectively. The Hartree-Fock single particle Hamiltonian $h[\rho]$ is related to the EDF, noted $E[\rho]$, by its first derivative $h[\rho](\mathbf{r}s q, \mathbf{r}'s' q') = \frac{\delta E[\rho]}{\delta \rho(\mathbf{r}'s' q', \mathbf{r}s q)}$.

B. Practical aspects

A TDHF calculation of two colliding nuclei is performed assuming that the two collision partners are initially at a distance D_0 in their HF ground state. This distance has to be big enough to allow Coulomb excitation in the entrance channel (polarization, vibration, rotation...). We chose $D_0 = 44.8$ fm in sections III and IV and $D_0 = 51.2$ fm in sections V. We assume that before to reach this distance, the nuclei followed a Rutherford trajectory which determines their initial velocities. A Galilean transformation [21] is then applied on each nucleus in the first iteration.

We use the TDHF3D code built by P. Bonche and coworkers with the SLy4d Skyrme parametrization [17]. This code has been extensively used to study heavy ion fusion [22, 23, 24, 25, 26, 27]. It has a plane of symmetry (the collision plane). It uses the Skyrme energy functional expressed in Eq. (A.2) of Ref. [28] where the

tensor coupling between spin and gradient has been neglected. The lattice spacing is $\Delta x = 0.8$ fm and the time step is $\Delta t = 1.5 \times 10^{-24}$ s.

III. FUSION AND TRANSFER IN LIGHT AND MEDIUM-HEAVY SYSTEMS

In this section, we focus on reactions with spherical nuclei. Studies of the effects of deformation on fusion within TDHF can be found in [23, 25, 26, 29].

A. Fusion barriers

Fusion barriers are classically defined as the energy threshold above which fusion occurs for a head-on collision. Experimentally, the average position of the barrier can be approximated by the centroid of the so-called barrier distribution [30]. To determine fusion barriers from TDHF, we consider head-on collisions at various energies. The barrier of a system is then located between the highest energy for which there is no fusion and the lowest one for which fusion occurs.

Figure 1 shows the density plot for a $^{16}\text{O}+^{208}\text{Pb}$ central collision at a center of mass energy $E_{CM} = 74.44$ MeV (top) and $E_{CM} = 74.45$ MeV (bottom). We see that the system separates into two fragments after a neck formation at the lowest energy. However, adding 10 keV is enough to fuse. We deduce the fusion barrier $V_B^{TDHF} = 74.445 \pm 0.005$ MeV for this system. This value is in excellent agreement with the experimental one $V_B^{exp} \simeq 74.5$ MeV [31].

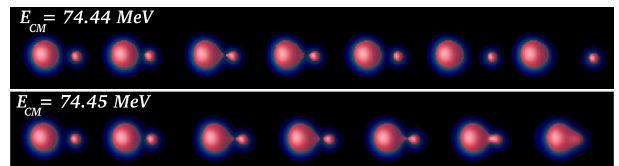


FIG. 1: Densities associated to a $^{16}\text{O}+^{208}\text{Pb}$ central collision at a center of mass energy $E = 74.44$ MeV (top) and 74.45 MeV (bottom). The surface corresponds to an isodensity at half the saturation density. Density decreases from red to black. Each plot is separated by 135 fm/c.

To see if these results are affected by dynamical effects, we compare them with a purely static approach. Figure 2 shows the nucleus-nucleus potential of this system if we assume frozen HF densities at various internuclear distances R using the same EDF and the same numerical approximations as in the TDHF calculations. Here, repulsion due to Pauli principle is neglected, which is a rather good approximation for distances down to the barrier as overlap of the nuclear densities are small. With this approach, the barrier is $V_B^{frozen} = 76$ MeV [27]. This is slightly higher than the TDHF value. This dif-

ference is due to dynamical effects such as transfer (see Section III B) that reduce the barrier.

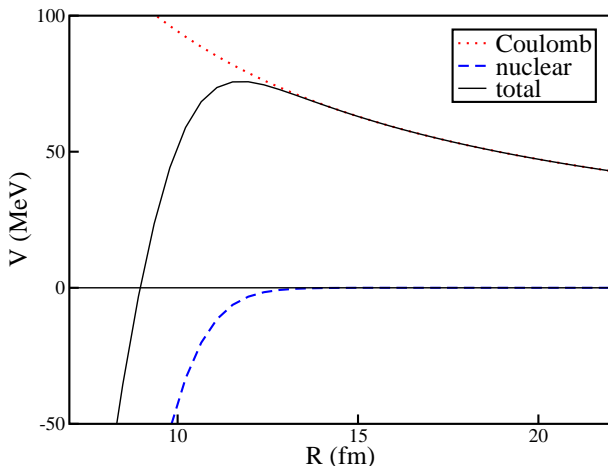


FIG. 2: Nucleus-nucleus potential of $^{16}\text{O}+^{208}\text{Pb}$ assuming frozen HF densities of the nuclei at various internuclear distances R .

Figure 3 shows a comparison between experimental fusion barriers and those from TDHF calculations for systems with various total masses and mass asymmetries. The lowest barrier is for $^{40}\text{Ca}+^{40}\text{Ca}$ and the highest one for $^{48}\text{Ti}+^{208}\text{Pb}$. The agreement with experimental data is slightly better with TDHF than with the Bass barrier [32]. Remembering that these TDHF calculations have no adjustable parameter on reaction mechanisms, we conclude that one can use it for fusion barriers predictions with confidence.

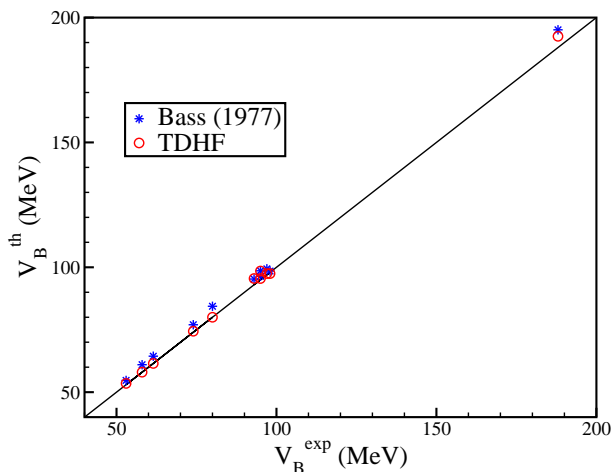


FIG. 3: Theoretical fusion barriers from TDHF calculations (circles) and the Bass barriers (stars) as function of the experimental values (from barrier distributions centroid).

B. Transfer below the barrier in $^{16}\text{O}+^{208}\text{Pb}$

It has been suggested that transfer may affect the barrier in the $^{16}\text{O}+^{208}\text{Pb}$ system [33]. Indeed, we see in Fig. 1 that the two fragments are linked by a neck and form a dinuclear system during ~ 400 fm/c. It is enough time for the nuclei to transfer nucleons, leading to a dynamical evolution of the barrier.

To get a deeper insight into the transfer preceding fusion in this reaction, we have plotted the evolution of the numbers of protons and neutrons of the small fragment as function of energy in Figure 4. Almost two protons and no neutron, in average, have been transferred from the ^{16}O to the ^{208}Pb . The two-proton transfer from the light to the heavy nucleus is then expected to be an important channel at the barrier. This is consistent with experimental observations of relatively high Carbon production cross sections, of the same order of the Nitrogen ones, in the exit channel of $^{16}\text{O}+^{208}\text{Pb}$ at the barrier [34, 35]. Note that we have to distinguish between the transfer of typically one or two nucleons and more violent collisions like deep-inelastic reactions. In the latter, the width of the particle number distribution is known to be underestimated with a single Slater determinant [36].

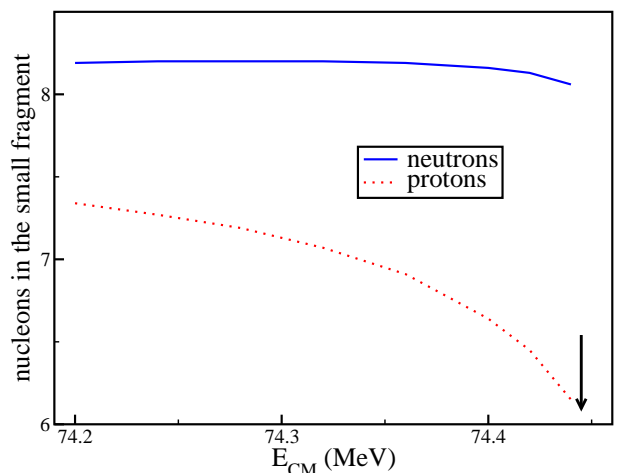


FIG. 4: Transfer below the barrier in $^{16}\text{O}+^{208}\text{Pb}$. The average number of protons and neutrons of the small fragment are plotted as function of energy. The arrow indicates the TDHF fusion barrier.

C. Fusion cross section of $^{16}\text{O}+^{208}\text{Pb}$

We now focus on fusion cross sections. In TDHF, the latter can be approximated by $\sigma_{fus}(E_{CM}) \simeq \pi b_c^2$ where b_c is the critical impact parameter associated to the initial Coulomb trajectory below which fusion occurs [26]. Figure 5 shows the excitation function obtained for the $^{16}\text{O}+^{208}\text{Pb}$ system in comparison to experimental data [31]. There is a good agreement above the barrier, though the fusion cross sections are overestimated

by about 16 %. The origin of this small discrepancy is nonetheless puzzling as the TDHF fusion barrier agrees perfectly with experiment. More precise investigations of fusion above the barrier with TDHF are then needed.

Below the barrier, the TDHF fusion cross section vanishes, following a classical behavior. This drawback of TDHF is well known and is due to the restriction to a single independent particles state. Indeed, to get a fusion probability between 0 and 1, we need at least two Slater determinants: one describing the two well separated fragments after the collision when fusion does not occur and one describing the fused system. It is necessary to go beyond TDHF to treat a sum of Slater determinants and then to describe sub-barrier fusion due to quantum tunneling.

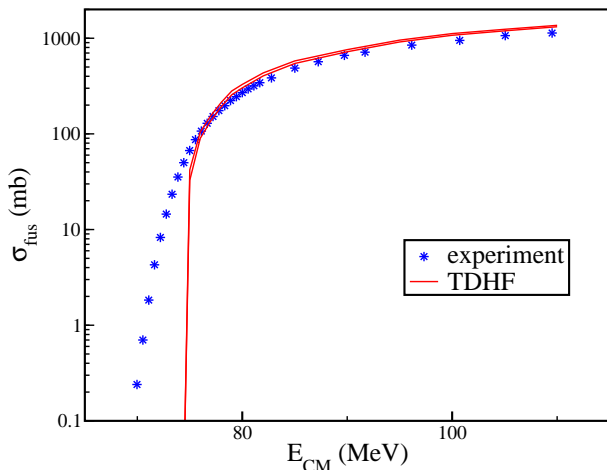


FIG. 5: Experimental fusion excitation function (stars) for $^{16}\text{O}+^{208}\text{Pb}$ from Ref. [31]. The lines denote the upper and lower limits for the fusion cross sections obtained from TDHF calculations.

IV. FUSION HINDRANCE OF QUASISYMMETRIC HEAVY NUCLEI

As we showed in the preceding section, TDHF systematics are in good agreements with experimental fusion barriers for light or medium-heavy systems. In these cases, models where the nuclei are assumed to be frozen with their ground state density give already a good approximation to fusion barriers. However, when collision partners get heavy and symmetric, typically when the product of their charges is such that $Z_1 \times Z_2 > 1600$, such frozen approaches significantly underestimate fusion barriers [4]. These systems need an extra energy to fuse compared to standard barrier height estimations. This phenomenon gave birth to the *extra-push* model [37]. One-body dissipation of the kinetic energy towards nucleonic degrees of freedom is often invoked to be responsible for this fusion hindrance. Thus, TDHF theory, which incorporates such one-body dissipation in the microscopic

description of nuclear dynamics, should be appropriate to study fusion mechanisms in heavy (quasi)-symmetric systems.

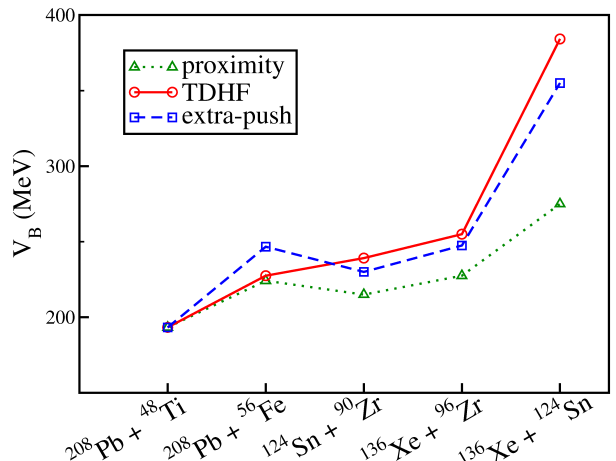


FIG. 6: Fusion barriers obtained for various systems with the proximity model [38] (dotted line), the extra-push model [37] (dashed line) and TDHF (solid line).

Let us now present a preliminary study of $^{48}\text{Ti}+^{208}\text{Pb}$, $^{56}\text{Fe}+^{208}\text{Pb}$, $^{90}\text{Zr}+^{124}\text{Sn}$, $^{96}\text{Zr}+^{136}\text{Xe}$ and $^{124}\text{Sn}+^{136}\text{Xe}$ head-on collisions. Due to computational time limitations, we assume that the nuclei have fused if a compact system is formed for a minimum duration of 1200 fm/c. Moreover, HF ground state of ^{124}Sn and ^{136}Xe are slightly deformed. As a first approximation, we neglect possible effects of deformation on fusion and consider only one orientation to limit computational effort.

Results are shown on Fig. 6, and compared with the extra-push model [37] and the proximity predictions of fusion barriers [38]. As we can see, TDHF results are in rather good agreement with the extra-push model. Both approaches predict significantly higher fusion barriers than the proximity model when mass symmetry increases. TDHF should then be useful tool to investigate dissipative mechanisms responsible for fusion hindrance.

Fusion models usually rely on the reduction of the complex dynamical many-body problem into few relevant degrees of freedom, like neck parameters, mass asymmetry or distance between fragments. The TDHF theory, however, is free of such choice of collective variables. Thus, the shape of the system can evolve freely in three dimensions. For example, we show on Fig. 7 snapshots of the density profile in the reaction plane of the $^{90}\text{Zr}+^{124}\text{Sn}$ central collision at $E_{CM} = 235$ MeV. This bombarding energy is 17 MeV higher than the barrier given by the Hartree-Fock frozen density approximation ($V_B^{frozen} = 218$ MeV) and 3.75 MeV below the TDHF fusion threshold ($V_B^{TDHF} = 238.75$ MeV). The separation of the system in two fragments is thus entirely driven by the fusion hindrance mechanisms.

We observe in Figure 7 the formation of a neck with a density close to saturation density. Also, this neck sur-

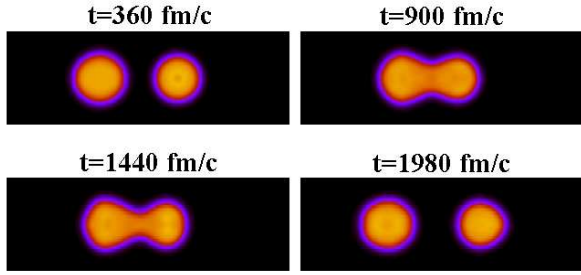


FIG. 7: Snapshots of the density profile in the reaction plane of the $^{90}\text{Zr}+^{124}\text{Sn}$ central collision at $E_{CM} = 235$ MeV. Hot colors are associated to densities close to the saturation density $\rho_0 = 0.16 \text{ fm}^{-3}$.

vives during approximately 1000 fm/c. This time is long enough to allow for a strong rearrangement of the system via nucleon transfer and dynamical shape evolution which modifies the fusion potential landscape. However, we also observe in Fig. 7 that this rearrangement is limited as it does not allow for the two fragments to merge and form a single one, i.e., the system keeps clearly the shape of a dinuclear system. These observations are encouraging and studies of isospin equilibration, mass transfer and shape evolution during the contact configuration are ongoing.

V. COLLISION TIME OF ACTINIDES

Collisions of two Uranium or heavier nuclei are used, amongst other things, to investigate the physics of super-strong electric fields [6]. Indeed, it has been proposed that a giant system with total charge $Z \geq 173$ may induce spontaneous electron-positron pair emissions from vacuum by a fundamental quantum electrodynamics (QED) process [5, 6]. However, no experimental evidence of this process has been obtained so far [39]. The keypoint might be a good understanding of collision dynamics, in particular a reliable prediction of collision times. In the $^{238}\text{U}+^{238}\text{U}$ reaction, one might be able to see this process for sticking times of several 10^{-21} s as shown by recent theoretical calculations based on the time-dependent Dirac equation [7].

Figure 8 shows that there is no pocket in the nucleus-nucleus potential of the $^{238}\text{U}+^{238}\text{U}$ system, in agreement with Refs. [40, 41]. However, dissipation mechanisms such as evolution of nuclear shapes may delay the separation of the system [42]. Experimentally, collision times have been estimated from oscillations in δ -electron spectra [43] and values of $\sim 2 \times 10^{-21}$ s have been obtained in $^{238}\text{U}+^{238}\text{U}$ above the barrier [44]. Recently, delay times in this reaction was searched analyzing kinetic energy loss and mass transfer [45]. On the theoretical side, macroscopic models have first been used (see, e.g., Ref. [42]). However, the complexity of reaction mechanisms and the

high number of degrees of freedom to be included in realistic calculations motivate the use of microscopic approaches. First microscopic calculations of the collision of two ^{238}U nuclei have been performed recently thanks to the Quantum Molecular Dynamics (QMD) model [41].

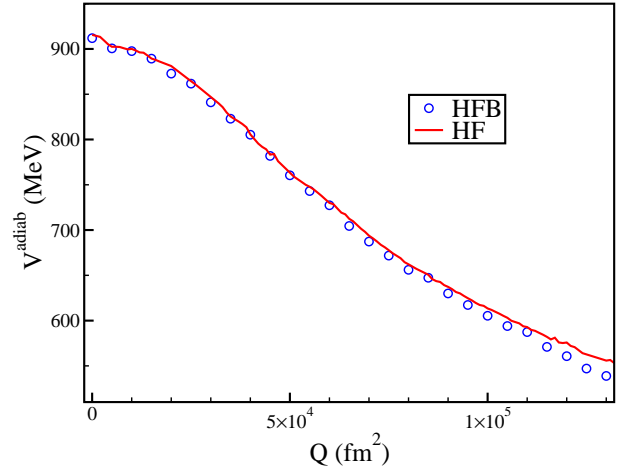


FIG. 8: Symmetric fission valley of the $^{238}\text{U}+^{238}\text{U}$ giant system. The Hartree-Fock (solid line) and Hartree-Fock-Bogoliubov (circles) adiabatic potential energies under a quadrupole constraint are plotted as function of the total quadrupole moment.

Here, we report preliminary results on central collisions of two ^{238}U with deformation axis parallel to each other and perpendicular to the collision axis. The collision time T_{coll} between nuclei is defined, here, as the time during which the neck density exceeds $\rho_0/10 = 0.016 \text{ fm}^{-3}$. Figure 9 shows the evolution of T_{coll} as a function of E_{CM} . We see a rise and fall of T_{coll} with a maximum of ~ 1000 fm/c at $1000 \leq E_{CM} \leq 1300$ MeV, in a rather good agreement with the QMD calculations of Ref. [41]. Central collisions in this energy range are then expected to produce superstrong electric fields with lifetimes which fill the necessary condition to observe e^+e^- pair excitations from QED vacuum.

VI. CONCLUSIONS AND PERSPECTIVES

We presented some applications of the TDHF theory to heavy ion collisions around the barrier. The only phenomenological input is the set of parameters of the energy density functional which have not been adjusted on any reaction mechanism. Despite this, the agreement between the TDHF calculations and the experimental fusion barriers is excellent for a wide range of projectiles and targets. However, these calculations overestimate the fusion cross sections for the system $^{16}\text{O}+^{208}\text{Pb}$ above the barrier by about 16%. Theoretical investigations are needed to understand this (rather small) disagreement.

Though the TDHF fusion cross section has a classical behavior, the quantum nature of the single-particle wave

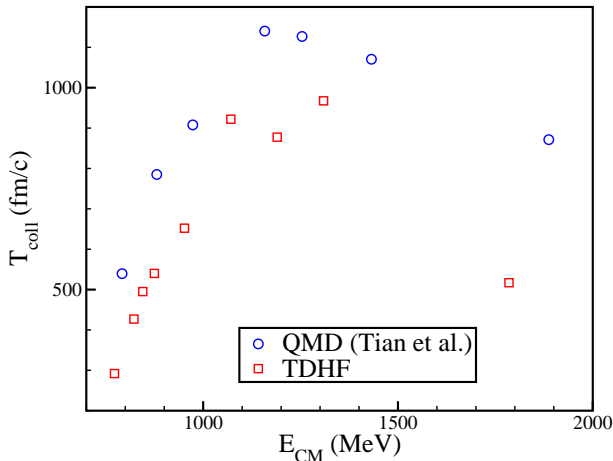


FIG. 9: Collision time of two ^{238}U nuclei as function of center of mass energy.

functions is well treated. Thus, we presented a study of transfer in the $^{16}\text{O}+^{208}\text{Pb}$ below the barrier. Two-proton transfer from the ^{16}O to the ^{208}Pb nucleus is dominant at the barrier. This qualitative observation is in agreement

with experiment.

We are presently extending the fusion study to heavy quasi-symmetric systems to investigate the phenomena responsible for the fusion hindrance in such systems. Preliminary results are encouraging as they indicate that this fusion hindrance is well reproduced by TDHF.

We finally presented calculations of collision times between two ^{238}U nuclei. Our conclusion is that the giant system might survive enough time (~ 1000 fm/c at an energy $1000 \leq E_{CM} \leq 1300$ MeV) to test nonperturbative quantum electrodynamics with super-strong electric fields.

Acknowledgements

We thank P. Bonche who provided his code. We are grateful to M. Dasgupta, R. Dayras, A. Drouart, W. Greiner, D. Hinde, D. Lacroix, W. Mittig, A. Villari and K. Washiyama for fruitful discussions. The calculations have been performed in the Centre de Calcul Recherche et Technologie of the Commissariat à l'Énergie Atomique.

-
- [1] M. Dasgupta, D. J. Hinde, N. Rowley, and A. M. Stefanini, *Annu. Rev. Nucl. Part. Sci.* **48**, 401 (1998), and references therein.
 - [2] S. Hofmann and G. Münzenberg, *Rev. Mod. Phys.* **72**, 733 (2000).
 - [3] D. J. Hinde *et al.*, *Phys. Rev. Lett.* **100**, 202701 (2008).
 - [4] H. Gaggeler *et al.*, *Z. Phys. A* **316**, 291 (1984).
 - [5] J. Reinhardt, B. Müller, and W. Greiner, *Phys. Rev. A* **24**, 103 (1981).
 - [6] *Quantum Electrodynamics of Strong Fields*, edited by W. Greiner (Plenum, New York, 1983).
 - [7] E. Ackad and M. Horbatsch, *Phys. Rev. A* **78**, 062711 (2008).
 - [8] P. A. M. Dirac, *Proc. Camb. Phil. Soc.* **26**, 376 (1930).
 - [9] D. R. Hartree, *Proc. Camb. Phil. Soc.* **24**, 89 (1928).
 - [10] V. A. Fock, *Z. Phys.* **61**, 126 (1930).
 - [11] T. Skyrme, *Phil. Mag.* **1**, 1043 (1956).
 - [12] D. Vautherin and D. M. Brink, *Phys. Rev. C* **5**, 626 (1972).
 - [13] M. Bender, P.-H. Heenen, and P.-G. Reinhard, *Rev. Mod. Phys.* **75**, 121 (2003).
 - [14] Y. M. Engel, D. M. Brink, K. Goeke, S. J. Krieger, and D. Vautherin, *Nucl. Phys. A* **249**, 215 (1975).
 - [15] P. Bonche, S. Koonin, and J. W. Negele, *Phys. Rev. C* **13**, 1226 (1976).
 - [16] J. W. Negele, *Rev. Mod. Phys.* **54**, 913 (1982).
 - [17] K.-H. Kim, T. Otsuka, and P. Bonche, *J. Phys. G* **23**, 1267 (1997).
 - [18] A. S. Umar and V. E. Oberacker, *Phys. Rev. C* **73**, 054607 (2006).
 - [19] E. Chabanat, P. Bonche, P. Haensel, J. Meyer, and R. Schaeffer, *Nucl. Phys. A* **635**, 231 (1998).
 - [20] B. Avez, C. Simenel, and Ph. Chomaz, *Phys. Rev. C* **78**, 044318 (2008).
 - [21] D. J. Thouless and J. G. Valatin, *Nucl. Phys.* **31**, 211 (1962).
 - [22] C. Simenel, Ph. Chomaz, and G. de France, *Phys. Rev. Lett.* **86**, 2971 (2001).
 - [23] C. Simenel, Ph. Chomaz, and G. de France, *Phys. Rev. Lett.* **93**, 102701 (2004).
 - [24] C. Simenel, Ph. Chomaz, and G. de France, *Phys. Rev. C* **76**, 024609 (2007).
 - [25] C. Simenel and B. Avez, *Int. J. Mod. Phys. E* **17**, 31 (2008).
 - [26] C. Simenel, B. Avez, and D. Lacroix, Lecture given at the Joliot-Curie school in Maubuisson (France, 2007), nucl-th/0806.2714.
 - [27] K. Washiyama and D. Lacroix, *Phys. Rev. C* **78**, 024610 (2008).
 - [28] P. Bonche, H. Flocard, and P.-H. Heenen, *Nucl. Phys. A* **467**, 115 (1987).
 - [29] A. S. Umar and V. E. Oberacker, *Phys. Rev. C* **74**, 024606 (2006).
 - [30] N. Rowley, G. R. Satchler, and P. H. Stelson, *Phys. Lett. B* **254**, 25 (1991).
 - [31] C. R. Morton *et al.*, *Phys. Rev. C* **60**, 044608 (1999).
 - [32] R. Bass, *Phys. Rev. Lett.* **39**, 265 (1977).
 - [33] I. J. Thompson *et al.*, *Nucl. Phys. A* **505**, 84 (1989).
 - [34] F. Videbæk *et al.*, *Phys. Rev. C* **15**, 954 (1977).
 - [35] E. Vulgaris, L. Grodzins, S. G. Steadman, and R. Ledoux, *Phys. Rev. C* **33**, 2017 (1986).
 - [36] C. H. Dasso, T. Døssing, and H. C. Pauli, *Z. Phys. A* **289**, 395 (1979).
 - [37] W. Swiatecki, *Nucl. Phys. A* **376**, 275 (1982).
 - [38] J. Blocki *et al.*, *Ann. Phys.* **105**, 427 (1977).
 - [39] I. Ahmad *et al.*, *Phys. Rev. C* **60**, 064601 (1999).
 - [40] J. F. Berger, J. D. Anderson, P. Bonche, and M. S. Weiss, *Phys. Rev. C* **41**, 6 (1990).

- [41] J. Tian, X. Wu, K. Zhao, Y. Zhang, and Z. Li, Phys. Rev. C **77**, 064603 (2008).
- [42] V. I. Zagrebaev, Yu. Ts. Oganessian, M. G. Itkis, and W. Greiner, Phys. Rev. C **73**, 031602(R) (2006).
- [43] G. Soff, J. Reinhardt, B. Müller, and W. Greiner, Phys. Rev. Lett. **43**, 1981 (1979).
- [44] R. Krieg *et al.*, Phys. Rev. C **34**, 562 (1986).
- [45] C. Golabek *et al.*, Int. J. Mod. Phys. E **17**, 2235 (2008).